



HYBRID OPERATION OF FUEL CELL AND PHOTOVOLTAIC BASED DGS

B.Venkatesh¹, M.Venkata Kirthiga²

^{1,2}National Institute of Technology, Trichy, Tiruchirappalli, Tamil Nadu

ABSTRACT

Owing to industrial and technological developments there has been a steep increase in the electric energy demand. Distributed Generation is being considered as a suitable alternative to solve this problem. In this regard, this paper focuses on the combined operation of two hybrid generators along with the utility grid to supply a common load. This work aims at an interconnected hybrid system with Solar Photo Voltaic (PV) based generator (season dependent) and Proton Exchange Membrane Fuel cell generator (dispatchable) to provide reliable and sustainable power to select loads. The solar energy is utilized to its utmost and the fuel cell is used as a back-up support unit. The nonlinear models for PEM fuel cell generator, power conditioning devices and controllers are designed and built in MATLAB/Simulink software and the integrated designs are validated. Hysteresis Current Controller is adopted for PEMFC and Maximum Power Point Tracking (MPPT) control algorithm for PV has been proposed. The overall scheme is investigated in open loop operation. Results show that the combined system delivers continuous power to the select load un-interruptedly.

Keywords—component; PEM Fuel cell, DC/DC Converter, VSI Inverter, PV System, Hysteresis control, Distributed Generator(DG)

I. INTRODUCTION

An ever increasing demand for electrical energy has brought renowned interest in renewable and sustainable power generation techniques. In densely populated countries, like India, there exists a dearth of power-generating resources, and the conventional centralized power generation units are not entirely capable of meeting the rising power demands. One of the potential solutions for these problems is to generate power in a distributed manner, making use of alternate energy resources, such as fuel cells, photovoltaic cells, wind turbines, and micro turbines [11].

Moreover, generation of power in a conventional manner requires combustion of hydrocarbon-rich fossil fuels such as coal, oil and natural gas. The combustion of these hydrocarbon-rich resources is proving to be dangerous for the environment, as it releases carbon dioxide/monoxide, one of the major anthropogenic greenhouse gases, in the earth's atmosphere, contributing to the effect of 'global warming'. The ill-effects of 'global warming' have been perceived worldwide by many researchers, and there exists a pronounced need to use alternative, more environmental-friendly power-generation methods which would not have any detrimental impact on the environment. The concept of 'green energy' has thus evolved based on the idea of generating electrical power

without any harmful impact on the environment and is realized using various technologies. The hydrogen-based resources, like fuel cells and micro turbines; renewable energy sources, like photovoltaic cells and wind power are the main sources of green energy.

Among the different sources, the season dependant sources are called non-dispatchable and the fuel operated sources are dispatchable. To ensure reliable and sustainable power supply to select consumers, it becomes inevitable to connect dispatchable and non-dispatchable sources to form hybrid generation systems. This work attempts at realizing one such hybrid system comprising of a PV system and Proton Exchange Membrane based fuel cell. Then sources are connected in conjunction with the utility to share a common load. The basic controllers used to orient the power flow in the hybrid system are also suggested in this work.

The photovoltaic (PV) system incorporates a Maximum Power Point Tracking (MPPT) technique to continuously deliver the maximum possible power to the load when there are variations in irradiation. The disadvantage of PV energy is that the PV output power depends on weather conditions and cell temperature, making it a non-dispatchable source. Furthermore, it is not available during the night. In order to overcome these inherent drawbacks, alternative source, such as PEMFC, should be installed in the hybrid system. By changing the FC output power, the hybrid source output becomes controllable [12]. This paper has tried to realize such a hybrid system.

The paper is organized as follows: Section-II deals with the hybrid system description. Section-III shows the Simulink models and results of the combined operation of the system. The paper concludes in section-IV.

II. SYSTEM DESCRIPTION

A. Model of Grid-Connected Hybrid Power System

The hybrid system constitutes combined operation of PV and FC sources along with utility grid in view of sharing a common load as shown in Fig. 1. The DC/DC converter connected at the PV is a cascaded boost converter which works as an MPPT controller. There are many MPPT algorithms proposed in the literature, such as Incremental Conductance (INC), Constant Voltage (CV) and Perturbation & Observation (P&O). The P&O algorithm has been widely used because of its simple feedback structure and fewer measured parameters [8]. The P&O algorithm is shown in Fig. 3.

B. Photo-Voltaic system model

The simple equivalent circuit has been adopted for the photovoltaic system as shown in Fig. 2. Since the density of solar radiation decides the magnitude of output power from the PV system a current source model is being adopted for PV generator.

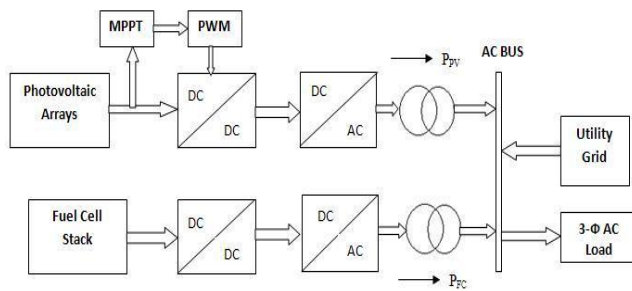


Fig. 1. Grid connected PV-PEMFC hybrid system

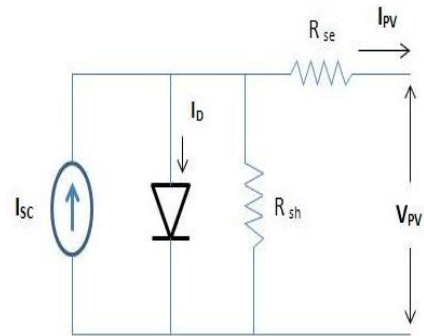


Fig. 2. Equivalent circuit of a PV cell

With reference to equivalent circuit, the PV panel current I_{PV} is expressed as:

$$I_{PV} = I_{SC} - I_D - I_{Sh} \tag{1}$$

$$I_{PV} = I_{SC} - I_0 \left[\exp \left[\frac{q(V + R_{se} I_{pv})}{nKT_k} \right] - 1 \right] - \frac{(V + R_{se} I_{pv})}{R_{sh}} \tag{2}$$

Assuming

$$\left[\exp \left[\frac{q(V + R_{se} I_{pv})}{nKT_k} \right] - 1 \right] \gg 1, \quad \frac{I_0}{I_{sc}} = 10^{-9}, \quad I_{ph} = I_{sc}$$

Now equation (2) is written as

$$I_{PV} = I_{SC} - I_D \tag{3}$$

$$\text{Where } I_D = 10^{-9} I_{SC} \left[\exp \left[\frac{20.7(V_{PV} + R_{se} I_{pv})}{V_{oc}} \right] \right]$$

C. Proton Exchange Membrane Fuel Cell Model

Owing to its high flexible control on dispatchable output power and efficiency of operation, PEM based fuel cells are most widely used in conjunction with non-dispatchable sources like solar generators. A detailed analytical model of PEMFC is shown in this section.

The open-circuit voltage of the PEM fuel cell is given as:

$$V_{O.FC} = n_s E_o^{cell} + \frac{n_s RT}{2F} \ln \left[\frac{P_{H2} \sqrt{P_{O2}}}{P_{H2o}} \right] \tag{4}$$

The actual terminal voltage of the PEM fuel cell at normal operating conditions is obtained by subtracting the voltage losses from the open-circuit output voltage of the PEM fuel cell as follows:

$$V_{fc} = V_{O.FC} - n_s (V^{act} + V^o) \tag{5}$$

The fuel cell system continuously consumes hydrogen and the reformer continuously generates hydrogen according to power demand. To model the reformer a second order transfer function as in equation (6) is developed [3]

$$\frac{q_{H_2}}{q_{methanol}} = \frac{CV}{T_1 T_2 S^2 + (T_1 + T_2)S + 1} \quad (6)$$

It is essential to control the hydrogen flow rate, in view of matching the power demand, in view of controlling the operation of a fuel cell system. A Proportional Integral (PI) controller is used in the system to control the hydrogen, oxygen, and water vapor flow rates. This feedback control is designed by taking the fuel cell output current and feeding it back to the input while converting the hydrogen into molar form based on equations (7)-(11).

The relationship between the hydrogen flow and the feedback current is represented as:

$$q_{H_2} = \frac{n_s I}{2FU} \quad (7)$$

The proposed PI controller is used to calculate the amount of hydrogen needed from the reformer which is used to determine the methane flow rate into the reformer. This is expressed as:

$$q_{methanol} = \left(K_3 + \frac{K_s}{T_3 S} \right) \left(\frac{n_s I}{2FU} - q_{H_2} + q_{methref} \right) \quad (8)$$

Mathematical representation of the oxygen flow rate is shown in (9)

$$q_{O_2} = \frac{1}{r_H - o} \quad (9)$$

In this model, dependency of the fuel cell operation upon the partial pressures of hydrogen, oxygen, and water vapor is introduced for the fuel cell stack. Some additional parameters adopted from the literature [4]-[7], are also used to get the model highly accurate and nonlinear. Following assumptions are made in the development of the model:

- The operating fuel cell temperature remains constant at 373K
- The reaction product entering the reformer is in the liquid phase
- The fuel cell stack output voltage is obtained by lumping together the individual cell parameters to represent a fuel cell stack
- Both the hydrogen and oxidants are humidified to prevent damage to the Proton Exchange Membrane

The mathematical representations of pressures of hydrogen and oxygen that are used in fuel cell output voltage equation are given as:

$$P_{H_2} = \frac{1}{K_{H_2}} \left(\frac{T_{H_2} S}{T_{H_2} + 1} \right) \quad (10)$$

$$P_{O_2} = \frac{1}{K_{O_2}} \left(\frac{T_{O_2} S}{T_{O_2} + 1} \right) \quad (11)$$

Irreversible voltage losses in the PEM fuel cell

Two types of voltage losses (drops) are considered in the model activation losses and ohmic losses. The governance of sluggish electrode kinetics by the rate of electrochemical reaction at an electrode surface gives rise to activation losses in the PEM fuel cell [7]. These losses are dominant at low current density (i.e. at the beginning of V-I characteristic curve of the PEM fuel cell). Expression for the activation voltage loss (drop) is given as [7]:

$$V^{Act} = \beta_1 + \beta_1 T + \beta_3 T \ln \left[1.97 * 10^{-7} P_{O_2} \exp \left(\frac{498}{T} \right) \right] + \beta_4 T \ln(I) \quad (12)$$

where the parametric coefficients are

$$\beta_1 = -0.948; \beta_2 = 0.00286 + 0.0002 \ln (A_{fc}) + 4.3 * 10^{-5} \ln (9.174 * 10^{-7} P_{H_2} \exp (-77/T)) ; \beta_3 = 7.6 * 10^{-5} ; \beta_4 = -1.93 * 10^{-4}$$

The ohmic losses are due to the ohmic resistance of the PEM fuel cell that includes the resistance of the anode and cathode due to imperfections in the electrode manufacturing and the resistance of the polymer electrolyte membrane to the movement of ions [7]. The expression for the ohmic voltage loss (drop) is given as:

$$V^o = \frac{181.6 \left[1 + 0.03 \left(\frac{I}{A_{fc}} \right) + 0.062 \left(\frac{T}{303} \right)^2 \left(\frac{I}{A_{fc}} \right)^{2.5} I \right]}{A_{fc} \left[11.866 - 3 \left(\frac{I}{A_{fc}} \right) \right] \exp \left[4.18 \left(\frac{T - 303}{T} \right) \right]} \quad (13)$$

D. MPPT Control

The two algorithms often used to achieve Maximum Power Point Tracking are the P&O and INC methods. The INC method offers good performance under rapidly changing atmospheric conditions. However, four sensors are required to perform the computations. If the sensors require more conversion time, then MPPT process will take more time to track the maximum power point. During tracking time, the PV output is less than its maximum power. This means that the longer the conversion time is, the large amount of power loss will be. That means if execution speed increases then the system losses will decrease. Moreover, this method requires two sensors, which reduces hardware requirement and cost.

To track the maximum power, two control methods that are often chosen are voltage-feedback control and power-feedback control [2]. Voltage-feedback control uses the solar array terminal voltage to control and keep the array operating near its maximum power point by regulating the array’s voltage and matching the voltage of the array to a desired voltage. The drawback of the voltage-feedback control is its neglect of the effect of

irradiation and cell temperature. Hence, the power-feedback control is used to achieve maximum power. The P&O MPPT algorithm with a power-feedback control is shown in Fig. 3.

E. Hysteresis current control

The system comprises of a three-phase inverter with a LCL-filter. The VSI consists of six Insulated Gate Bipolar Transistors (IGBT)s with an anti-parallel diode across each device. A PI controller in series with a hysteresis block implements the current control of the VSI. This is shown in Fig. 4.

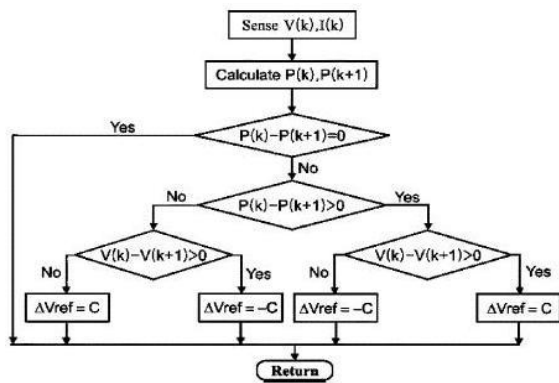


Fig. 3. P&O MPPT algorithm

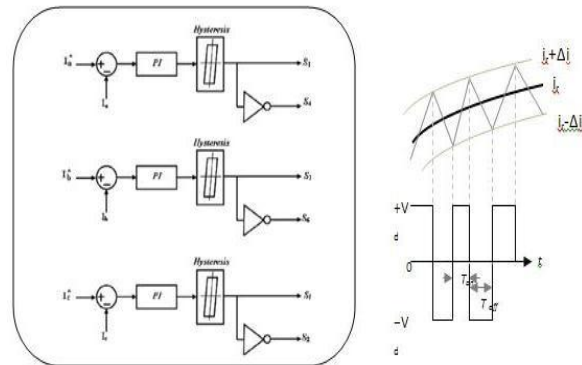


Fig. 4. Proposed current control scheme

The main function of a VSI controller is to sense a load demand and to provide a feedback current to fuel cell reformer to determine how much to send forward to the fuel cell stack. IGBT switches are used in three legs. A PI-controller in series with a hysteresis block implements the current control of the VSI. The objective of the controller is to force the inverter output current to track the reference current that is derived from the grid voltage [7]. The current control is achieved by comparing a reference current signal with actual inverter output current, thus generating an error signal. The error signal is processed by a PI controller. The output of the PI controller is fed to a hysteresis current controller. The real power is controlled by varying the magnitude of the reference current signal. The rigid band hysteresis current controller switches the power circuit to maintain the current between upper and lower bound values [8]. Whenever the error reaches one of the two values, the power circuit is switched so that the current begins to move backwards in other direction. In this way, the current is controlled to stay between two bounded values. The output of the hysteresis block is the gating signal, which is fed to the driving circuit.

III. SIMULINK MODELS AND RESULTS

A. Fuel cell generator

In this mode PEM Fuel cell generator is used along with the fuel cell reformer. The feedback current (load current) is changed in regular time intervals and corresponding changes in fuel cell voltage and pressures of fuels are examined [3]. For a time interval of $0 < t < 20$ sec, 10A current is applied and during $10 < t < 50$ sec, 30A current and for $50 < t < 100$ sec, 20A current is applied at the feedback terminals. The Fig. 5 shows the Simulink model of fuel cell generator with fuel reformer and individual blocks are shown in Fig. 6 and Fig. 7

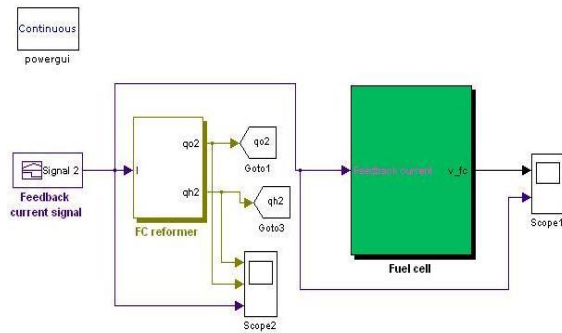


Fig. 5. Model of fuel cell generator with fuel reformer

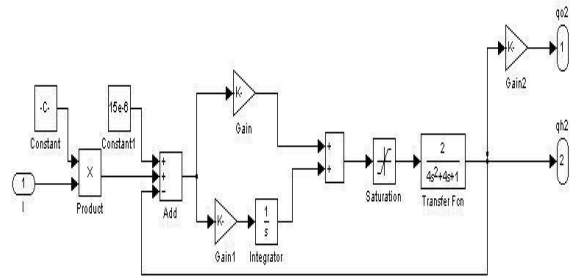


Fig. 6. Simulink model of fuel reformer

Fuel cell generator model shown in Fig. 5 is tested with step changes in feedback current. The results of the simulation show that as the feedback current increases fuel cell voltage decreases. The increase in current increases the hydrogen and oxygen flow rates as well. All three signal variations incorporate a small time delay before attaining steady state. Response of the partial pressures of H₂ and O₂ as well as the reformer with respect to change in current is shown in Fig. 8 and Fig. 9.

The Fig. 10 shows the variation in fuel cell output voltage when the feedback current is varying up to the rated value (30A). For the time period of 0 < t < 20 sec current is 10A; for 20 < t < 35 sec current is 20A; for 35 < t < 50 sec current is 30A (Rated current); for 50 < t < 70 sec current is 5A.

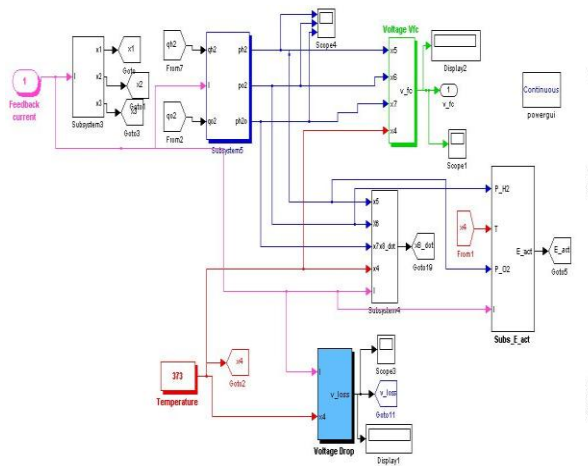


Fig. 7. Simulink model of PEM fuel cell

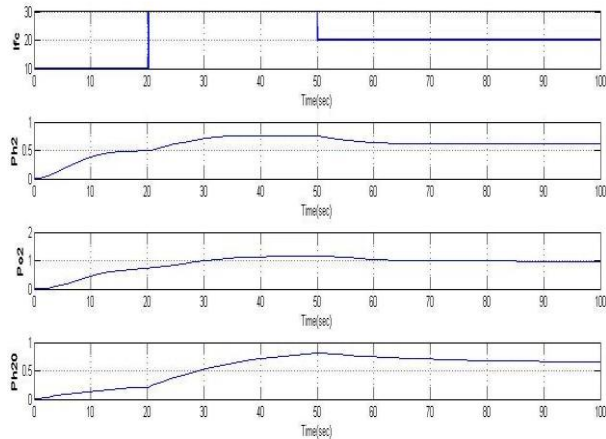


Fig. 8. Variation in P_{H2}, P_{O2} with respect to change in current

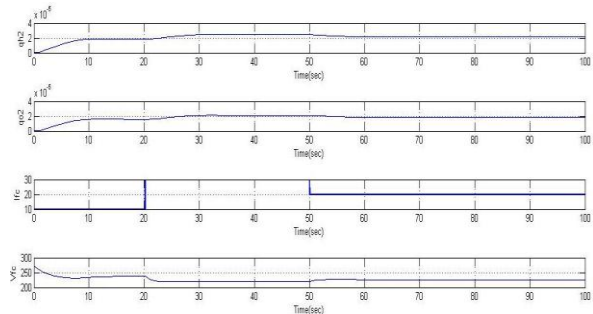


Fig. 9. Reformer response to change in current

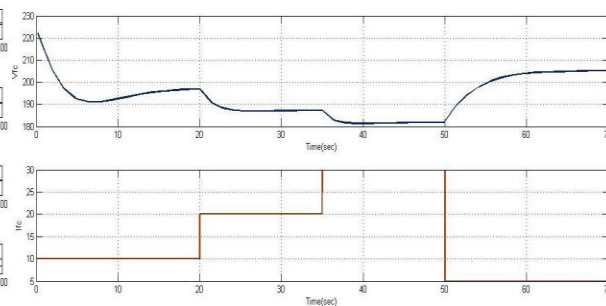
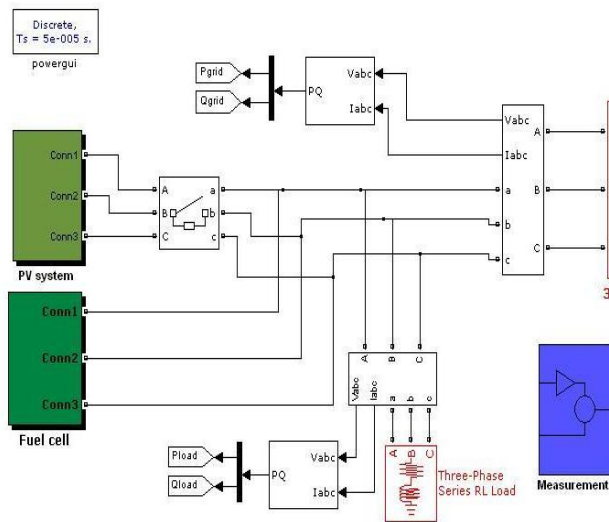


Fig. 10. Response of Fuel cell output voltage to change in current

B. Combined operation of fuel cell & photovoltaic based DGs

The work focuses on the integration of PhotoVoltaic (PV) and Fuel Cell (FC) systems for sustainable power generation. A hybrid system with PV and FC is formed and controlled as open loop operation. Usually in a hybrid system, renewable energy based resource is given first priority in view of improving the fuel economy of the dispatchable source. In this work it is considered that solar radiation is available to a limited period. Hence fuel cell is considered as a main back-up source. During adequate insolation MPPT controller draw maximum power from the photovoltaic source. Hence no battery system is required here. When solar insolation is not available, fuel cell is used to supply the customer. The FC system has 6 KW capacity while the PV panels used in this model are capable of delivering 2.5 KW at best radiation conditions. The Simulink model is shown in Fig. 11 and the various parameters of the sources are given in Table I & Table II

TABLE I Configuration parameters of PEMFC DG



| Name | Parameters | Rating |
|----------------------|---|-------------------------------|
| Fuel cell generator | Power rating Open-circuit voltage No. of cell in stack Stack temperature | 6 kW 320 V 248 373 K |
| Boost converter | Power rating Proportional gain Integral gain | 6kW, 200V/400V 0.01 0.1 |
| Three phase Inverter | IGBT switch | 400VDC/312V AC |
| LCL Filter | Inductor Capacitor | 2mH 1µF |
| Grid | Line-line voltage Line frequency | 440V(RMS) 50 HZ |

Fig. 11. Grid connected integrated model of PV and PEM fuel cell DG

Integrated system is simulated for 2 sec. System reaches steady state after 0.4 sec and then reference powers of PEM Fuel cell plant is varied in the order of 5 kW, 4 kW, 3kW and 4kW for every 0.4 sec time duration of 2 sec. But Solar PV system power is fixed by keeping the radiation at 800 W/m² and is operated for particular time duration to show the load sharing between two renewable sources. Total load on the system is fixed at 12kW and the hybrid system is controlled to supply the load. Solar PV system is ON for period of 1.2 < t < 1.6 sec. During that time grid power is reduced. This indicates that power sharing between two DGs is obtained. Load sharing among two DGs are indicated in Table 3.

Fig. 12 shows the power sharing among two distributed generators. Fig. 13 & 14 shows the power, voltage and current waveforms of solar PV system and PEM Fuel cell system respectively.

TABLE II Parameters of PV module

| Parameter | value |
|------------------------------------|----------------------|
| Maximum power of the single module | 80 W |
| Standard Temperature | 25 °C |
| Standard Irradiation | 800 W/m ² |
| Open circuit voltage | 203.9 V |
| Short circuit current | 16.54 A |
| Number of strings in parallel | 4 |
| Number of panels in series | 10 |
| Maximum Power rating | 2.4 kW |

TABLE III Load sharing between two DGs (Load demand 12 KW)

| Time (sec) | PEMFC Generator power output (KW) | PV system power output (KW) | Grid output power (KW) |
|---------------|-----------------------------------|-----------------------------|------------------------|
| 0 < t < 0.8 | 5 | 0 | 7 |
| 0.8 < t < 1.2 | 4 | 0 | 8 |
| 1.2 < t < 1.6 | 3 | 2.3 | 6.7 |
| 1.6 < t < 2 | 4 | 0 | 8 |

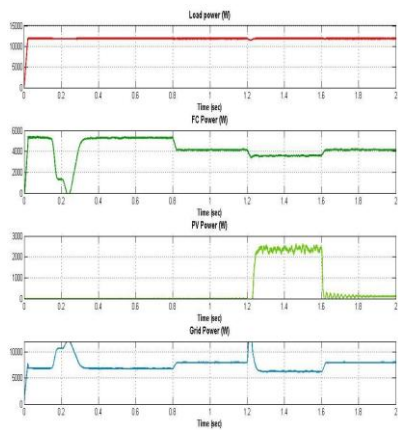


Fig. 12. Active power waveforms current waveforms of

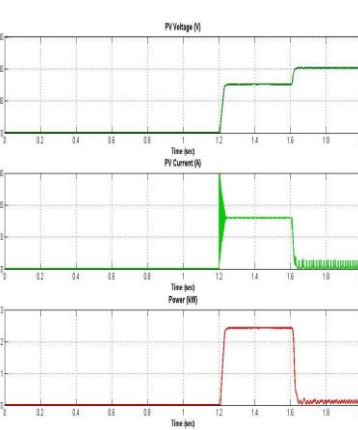


Fig. 13. Voltage & current waveforms of PV

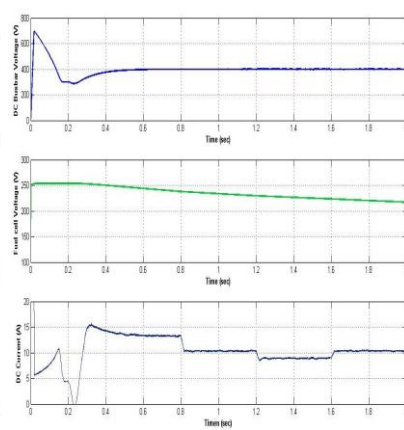


Fig. 14. Voltage and

PEM fuel cell generator

IV. CONCLUSIONS

In this paper combined operation of PEM Fuel cell based DG (dispatchable) and a Solar Photovoltaic based DG (non-dispatchable) is mimicked for its operation in grid connected mode of operation. A detailed nonlinear modeling of PEM Fuel cell with power conditioning devices such as boost converter and a three phase inverter is attempted. PV source is supplemented with a dedicated MPPT controller and a Hysteresis Current Controller is dedicated to the PEMFC source in this work. The controllers show substantial contribution in getting a steady output from the utility grid.

PV module is tested at different insolation values and is designed to give maximum power at all conditions when integrated with grid. Fixed load conditions are investigated and the sources are made to share the load. Whenever solar irradiation is available it is made use to its utmost. The fuel cell source is used as back-up source as it is dispatchable.

Inspite of these advantages, the proposed scheme is not synchronized and no coordinated control between two DGs has been addressed in this work. These can be developed as a future scope of this attempt.

APPENDIX

| Parameter | value |
|--|------------------------------|
| Number of cell used (n_s) | 248 |
| Faraday's constant (F) | 96484600C kmol ⁻¹ |
| Universal Gas Constant (R) | 8314.47 |
| Utilization Factor (U) | 0.8 |
| Reformer Time Constant (τ_1) | 2 |
| Reformer Time Constant (τ_2) | 2 |
| PI Controller Time Constant (τ_3) | 2 |
| Conversion Factor (CV) | 2 |
| Methane Reference Signal ($q_{methref}$) | 15*e-6 |
| Hydrogen-Oxygen Flow Ratio (r_{H_2O}) | 1.168 |
| Hydrogen Valve Constant (KH ₂) | 422*e-7 |
| Oxygen Valve Constant (KO ₂) | 211*e-7 |
| Water Valve Constant (KH ₂ O) | 7716*e-9 |
| Hydrogen Time Constant (τ_{H_2}) | 3.37 |
| Oxygen Time Constant (τ_{O_2}) | 6.74 |
| Water Time Constant (τ_{H_2O}) | 18.418 |
| Standard No-Load Voltage (E_0^{cell}) | 0.8 |
| PI controller gain (K_3) | 0.25 |
| Stack Temperature (T) | 373K |
| Area of single fuel cell (A_{fc}) | 232 cm ² |

REFERENCES

- [1] Sachin V. Puranik, Ali Keyhani and Farshad Khorrami, "State-Space Modeling of Proton Exchange Membrane Fuel Cell," *IEEE Transactions on energy conversion*, Vol. 25, No. 3, September 2010.
- [2] O.C.Onar, M.Uzunoglu, M.S.Alam, "Dynamic modeling, design and simulation of a PV/FC/UC based hybrid power generation system," *Journal of power sources* 161(2006).
- [3] Sukumar kamalasadnan, "Modeling and Simulation of PEM Fuel Cell as a Micro grid," *IEEE Trans. Power systems*, Vol.19, issue 4, pp 2022-2028, November 2004.
- [4] C.Wang, M.H.Nehrir, "Control of PEM Fuel cell Distributed generation systems", *IEEE Transactions on Energy conversion*, Vol.21, No.2, June 2006.
- [5] S.Pasricha and S.R.Shaw, "A dynamic PEM fuel cell model," *IEEE Trans. Energy Convers.*, Vol.21, No.2, pp 484–490, Jun.2006.
- [6] W.Friede, S.Rael, and B.Davat, "Mathematical model and characterization of the transient behaviour of a PEM fuel cell," *IEEE Trans.Power Electron.*, Vol.19, No.5, PP.1234–1241, Sep.2004.
- [7] J. Kim, S. Lee, S. Srinivasan, C.E. Chamberlin, "Modeling of Proton Exchange Membrane Fuel Cell Performance with an Empirical Equation," *Journal of Electrochemical Society*, Vol. 142 No. 8, August 1995, PP. 2670-2674.
- [8] H.Habeebullah Sait, S.Arul Daniel, "New control paradigm for integration of photovoltaic energy sources with utility network," *Electrical Power and Energy Systems journal* 33 (2011) 86–93.



- [9] McMurray. W, “Modulation of the chopping frequency in dc chopper and PWM inverters having current-hysteresis controllers,” *IEEE Trans Ind Appl* 1984;20(4):763–7.
- [10] Malesani. L, Tenti. P, “A Novel Hysteresis control method for current controlled voltage-source inverter with constant modulation frequency,” *IEEE Trans Ind Appl* 1998;26(1):88–92.
- [11] S.G. Tesfahunegn, P.J.S. Vie, Tore M. Undeland, “A Combined Steady State and Dynamic Model of a Proton Exchange Membrane Fuel Cell for use in DG system Simulation,” *The 2010 International Power Electronics Conference*.
- [12] EG&G Services, Inc., Science Applications International Corporation, “*Fuel Cell Handbook* (Sixth Edition),” *Office of Fossil Energy, National Energy Technology Lab, Nov. 2002*.
- [13] Wei Wu, Che-Chuan Pai, “Modeling and Control of a Proton Exchange Membrane Fuel Cell System with Alternative Fuel Sources,” *Ind. Eng. Chem. Res.* 2009, 48, 8999–9005.